Microfluidic patterning of alginate hydrogels

Robert M. Johann[a)]
Fraunhofer-Institute for Biomedical Technology (IBMT), D-66386 St. Ingbert, Germany

Philippe Renaud[b)]
Swiss Federal Institute of Technology, EPFL-STI-LMIS, CH-1015 Lausanne, Switzerland

In this article the authors present techniques which allow the microfluidic design of alginate microgels with layer composition on a chip. The hydrogel is created by combining two laminar flows of the gel precursor solutions—a calcium solution and an alginate solution—in a microchannel. The alginate solution is loaded with particles and by employing a certain fluid handling protocol involving several alginate solutions with different types of particles, a gel bar composed of many layers, each layer filled with a certain particle type, is formed. This method allows to produce defined lamellae of gel with extraordinarily small size and large aspect ratios. The minimal width attainable for a single layer by this technique is determined by the experimental conditions and for the conditions of the present article layer widths on the order of 10 μm have been realized at a gel thickness of 100 μm. Another method described is based on the finding that the degree of particle incorporation in the gel varies with the particle speed in the alginate flow. Altering the alginate flow rate thus allows to form a gel bar with an inner structure due to varying particle density. The authors believe that alginate gel patterning technology, which relies on easily available equipment and involves gentle particle immobilization conditions, could offer a novel approach toward the engineering of artificial tissues on the micrometer range or to cell micropatterning for analytical purposes. © 2007 American Vacuum Society. [DOI: 10.1116/1.2746873]

I. INTRODUCTION

Hydrogels represent a class of polymers that is characterized by a high water content, a loose, porous polymer network, and concomitant low mechanical strength. An interesting physical property of hydrogels resulting from this structure is the response to changes of solvent, ionic strength,[1] pH,[2,3] electric field,[4] temperature,[5] or light[6] by a reversible expansion or shrinkage of volume. This effect is utilized in efforts to produce artificial muscles[7] or for autonomous valves in fluidic systems.[2,8] Thermoresponsive hydrogels are used for pumping, metering, and flow regulation in microfluidic chips.[9,10] Other microfluidic systems utilize porosity and high flow resistance of the gels for analytical applications such as dialysis,[11] electrophoresis,[12–15] substance enrichment,[16,17] and sample separation by a combination of electrokinetic and hydrodynamic flows.[18] Hydrogels are also used as encapsulation matrices for microfluidic enzyme bioreactors and sensors.[19–21]

A very important field for the application and investigation of hydrogels is the engineering of artificial tissues. Hydrogels are considered very appropriate to the synthesis of artificial tissue scaffolds due to the structural similarity to their natural counterparts, their capability of encapsulating cells under mild conditions, and the amenability to chemical modification.[22,23] Embedding cells in a hydrogel offers the opportunity to compare cell behavior on three- with that on two-dimensional substrates, where there is evidence for a difference.[24,25] Natural tissues usually have an inner structure which is required for their peculiar function, and methods enabling to reproduce those structures within hydrogels with embedded cells are therefore highly useful.

A few concepts have been developed very recently which allow to pattern a coherent piece of hydrogel containing cells on the order of 100 μm using microfluidic devices. Albrecht et al.[26] reported the fabrication of a thin gel sheet with heterogeneous composition and enclosed cells by photopolymerization in several steps. Burdick et al.[27] and Zaari et al.[28] produced a hydrogel with continuous distribution of embedded particles or molecules using a microfluidic gradient generator and photopolymerization. Other authors described the formation of vertically stacked layers by polymerizing parallel laminar flows[29] or by repeatedly filling a microchannel with a hydrogel that shrinks on solidification.[30]

Here we present methods which enable the micropatterning of particles in a thin bar of alginate gel on a microfluidic chip. Gel formation is based on the controlled manipulation of laminar flows of an alginate and a calcium solution on a chip according to a previously published technique.[31] The gelling of alginate is induced by chemical reaction with calcium (and other metal ions) even with very low calcium concentrations in the absence of UV light or heat. The harmlessness of the employed substances and conditions and the possibility of easily dissolving the gel make this method very suited for the temporary encapsulation of cells, for which it is widely employed. In the first approach a microgel bar is constructed by attaching a number of individual layers of gel applying an iterative flow switching procedure. The variability in composition of the layers is not limited. Filling each

---

[a)]Electronic mail: robert.johann@ibmt.fhg.de
[b)]Electronic mail: philippe.renaud@epfl.ch

layer with a different particle sort results in a gel bar assembled of many fine lamellae, which are well defined and can have exceptionally small widths and large aspect ratios. The second method of gel structuring relies on the observation that the degree of particle incorporation into the gel is a function of the speed of the particle carrying flow. Utilizing this effect a gel bar has been patterned with one particle sort by flow rate variation.

II. EXPERIMENT

A. Materials

Sodium salt of alginic acid (from Macrocystis Pyrifera), calcium chloride dihydrate, disodium ethylenediaminetetraacetic acid (EDTA), sodium chloride, and 50% (w/v) poly-(ethyleneimine) (PEI) (M_w, 750 000) solution in water were purchased from Sigma-Aldrich. Colored flow separation buffer was prepared by mixing blue food dye (E131) with water (approximately 3:1 for the used channel height). The dye (E131) and baker's yeast (*Saccharomyces cerevisiae*) were bought in a local grocery. All substances were used as received. 2 μm large blue fluorescing polystyrene beads and 5.14 μm green fluorescent beads were obtained from Duke Scientific, and 4 μm beads with red fluorescence from Molecular Probes.

For gel fabrication 2% (w/w) alginate solution in water was used. The solution was prepared by dissolving the alginate salt in boiling water and stored in the refrigerator at 4 °C. Before use it was filtered through 0.2 μm pore size syringe filters. Beads were added to the alginate solution in the concentrations of 1.1×10^8 beads/ml for the 2 μm sized beads, 2.8×10^7 beads/ml for the 4 μm sized beads, and 6.5×10^6 beads/ml for the 5.14 μm sized beads. Calcium chloride solution was applied with 20 or 40 mM concentration for alginate polymerization. Gels were dissolved using aqueous 0.2 mM EDTA solution.

B. Microchip design

The component parts of the used chip are shown in Fig. 1(a). For the "plug-and-play" connection of fluid supply tubes, a 5 mm thick slab of polydimethylsiloxane (PDMS) (Sylgard 184, Dow Corning) (A) with punched via holes was oxygen plasma bonded to a 1 mm (40×26 mm^2) thick piece of float glass (B), which was cut from a standard microscope slide (Menzel-Gläser) and provided with mechanically drilled fluid access holes. The channel layout, which is shown in Fig. 1(b), was cut in a 100 μm thin membrane of PDMS (C). The membrane was prepared by spin coating the prepolymer on a flat scratch-free surface of a polystyrene plate, which allowed us to easily peel off the membrane after curing. To avoid deformation of the plastic, the PDMS was cured at 60 °C for 1 day. A piece of the membrane was cut and placed on a clean thin cover slide (Esco, Erie Scientific) (D). For transferring and cleaning the membrane, it may help to spread it out on a water surface. Then the cover slide with the membrane was laid on a printed paper template with the channel layout, and the contour was cut into the membrane
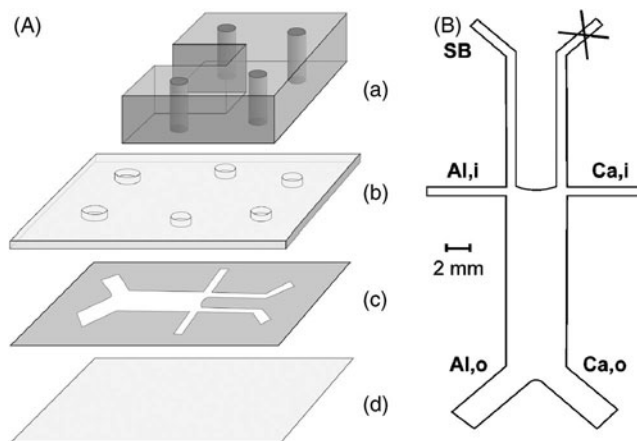

FIG. 1. (a) Microchip design. (A) PDMS interface, (B) glass plate with fluid access holes, (C) PDMS membrane with channel cut, and (D) cover slip. (b) Channel layout with separation buffer inlet (SB) and the inlet and outlet for the calcium (Ca,i; Ca,o) and the alginate solutions (Al,i; Al,o).

under the microscope using a scalpel. The manual cutting was sufficiently accurate because of the large channel widths employed, which are on the order of a millimeter. Finally, the cover slide with the membrane was aligned and pressed onto the float glass plate after cleaning of the surfaces. Bonding between the PDMS membrane and the glass plates was achieved through conformal contact and proved to be so durable and strong that leakage was never observed and the cover slide could not be detached without breaking. This chip manufacture demands some skill, but it is doable at low cost and with standard laboratory equipment delivering a very robust microdevice.

The use of the inlets is indicated in the layout of Fig. 1(b). The notations will be used in the following text. SB is the inlet for the blue dye separation buffer; the entrance on the opposite side of the symmetric layout is plugged. On the side of the buffer inlet there are the inlet (Al,i) and the outlet (Al,o) for the alginate solutions; on the opposite side there are the corresponding openings for the calcium solution, (Ca,i) and (Ca,o).

C. Channel treatment

A typical feature of hydrogels is their weak adhesion to surfaces. Also the adhesion of calcium alginate gel on glass is weak. However, in order to be able to control the gel growth and to avoid uncontrolled reaction between alginate and calcium by leakage flows between the gel bar and the glass walls on bottom and top, it is necessary that the formed gel tightly adheres to the channel walls. The rigid chip construction (Fig. 1) is expected to promote the adhesion of the gel in the channel and to minimize leakage flows. The adhesion of the alginate gel to the glass is strongly improved by coating the channel surfaces. The channels were first coated with a layer of PEI by filling the chip with a solution of 0.5 wt % PEI and $1M$ NaCl in water after oxygen plasma treatment of the dried chip. In multilayer deposition techniques PEI is often used as the first layer to mediate the

adhesion of the following layers on the substrate.[32,33] The solution was left to stand in the chip for at least 30 min. Afterward, the channels were rinsed with water, and a 1 wt % alginate solution was introduced and left to stand for the same time. Alginate is a negatively charged polymer and expected to deposit on the positively charged PEI.[33,34] The gel will polymerize and adhere on the outer alginate surface layer by means of the calcium ions. Firm attachment of the gel to the glass is indicated from the stable position of the gel bar and a regular and reproducible shape, which is determined by the diffusion controlled reaction between calcium and alginate.[31] When gel adhesion is weak, bending and shifting of the gel bar is observed in the initial phase of gel formation, and leakage flows between gel and channel walls result in an irregular gel shape (videos 1–3 of the supporting information).[39] The surface treatment assures strong gel adhesion for about five gel productions, before it has to be renewed. Evidently, the polymer layer is degrading with each gel formation and dissolution process.

D. Gel formation

Formation and subsequent dissolution of an alginate gel bar encapsulating yeast cells on a chip is shown in Fig. 2. In the beginning three parallel laminar flows of calcium solution [inlet (Ca,i) in Fig. 1(a)], alginate solution (Al,i), and colored liquid (SB) are set up in the central channel [Fig. 2(a)]. The SB is in the middle and serves to keep the prepolymer flows separate and be a visible guide for adjusting the flows. In this case the SB contains EDTA to enable also gel dissolution without using a new liquid. Due to the viscosity of the alginate solution, the flows need a certain time to stabilize. The fluids are driven by pressure, which is regulated independently for the three inlets by using three commercial pressure reducers connected to a laboratory gas tap. The flows are adjusted such that no portion of the calcium stream is leaving except the outlet (Ca,o), also the outlet channel (Al,o). Since the gel grows into the alginate flow, this may result in the blockage of the outlet (Al,o). Then the separation flow is switched off. Upon contact of the prepolymer flows, the gel starts to grow at the border of the two laminar flows [Fig. 2(b)]. By exchanging the alginate for the SB/EDTA solution, gel growth is interrupted [Fig. 2(c)] and the gel bar is dissolved completely [Fig. 2(d)]. The embedded cells are released and returned into the liquid. Afterward, a new gel can be formed in the same channel again. When the gel is firmly attached in the channel, regular gel bars with uniform width are obtained [Figs. 2(b) and 2(c)]. Slightly wedge shaped gels as the one presented in Fig. 1(d) of Ref. 31 can be attributed to the ion depletion of EDTA in the alginate flow down the channel.

E. Image analysis

Image sequences for evaluating gel growth were acquired with a QICAM camera (cooled, 10 bit, Quantitative Imaging Corporation) using VIDEO SAVANT 4 (Io Industries) as the camera interface software. The frames captured periodically were processed in ADOBE PHOTOSHOP for measuring gel
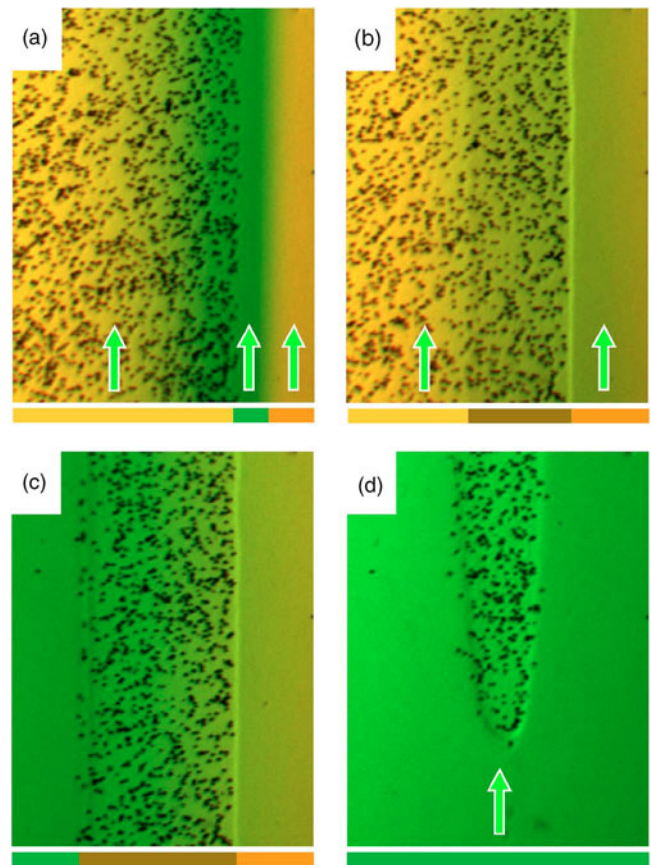

FIG. 2. Formation of an alginate microgel bar with embedded yeast cells on a chip. (a) Parallel laminar flows of an alginate solution with cells, a calcium solution, and colored separation buffer (here with EDTA) are introduced in a microchannel (the arrows indicate the flow direction). (b) Gel formation between the alginate and the calcium flow is induced upon removal of the buffer flow. (c) Gel growth is stopped and (d) immediately dissolved by introducing the blue EDTA solution. (yellow) Sodium alginate solution with yeast cells, (green) colored separation buffer solution with EDTA, (orange) calcium chloride solution, and (brown) calcium alginate hydrogel. Size of an image: $530 \times 700 \ \mu m^2$.

widths. The average velocity of the particle carrying flow was approximated from particle velocities.

III. RESULTS AND DISCUSSION

A. Gel patterning by fluid exchange

The fluidic setup for creating layered microgels is presented in Fig. 3(a). The liquids are supplied by pressure from gas tight reservoir vessels. The setup corresponds to that for the formation of homogeneous gel bars according to the procedure described above, except that instead of a single alginate solution several vessels with different compositions are used, which are connected to the same pressure. The solutions are exchanged by means of a multiport rotary valve. To minimize the exchange time with the present setup, the distance between the valve and chip inlet is chosen as small as possible (≈ 4 cm) and a small inner diameter tube ($\approx 250 \ \mu m$) is used. The fluids are allowed to exchange for at least 20 min, in order to rinse out all the particles from the former alginate/bead solution. A modified chip layout, where
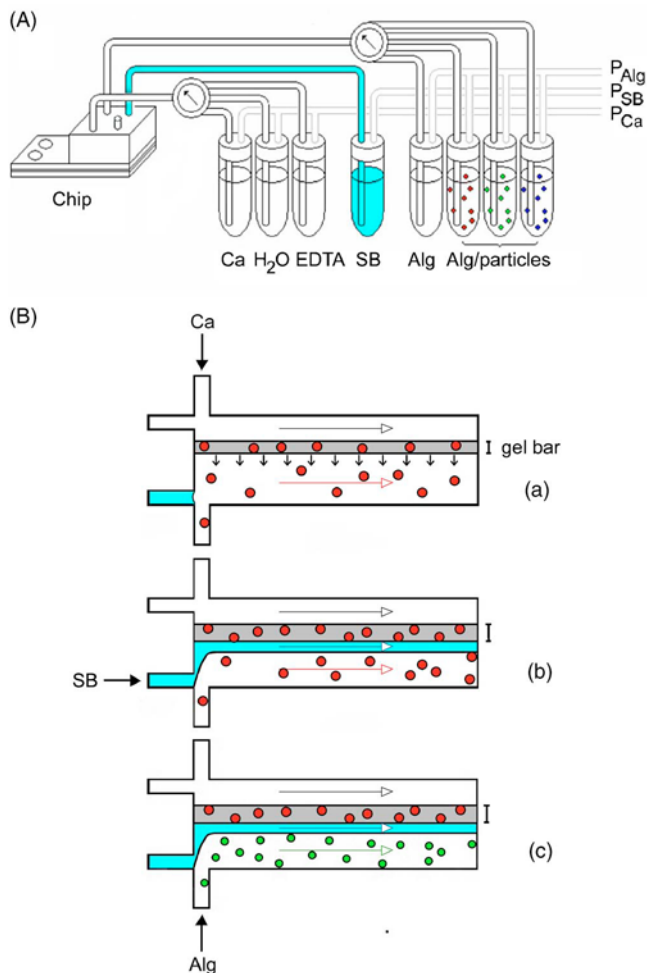
(A)

Chip

Ca H₂O EDTA SB   Alg Alg/particles

(B)

FIG. 3. (a) Fluidic setup for preparing layered microgels. H₂O represents a cleaning solution, and P_i the pressure inlets. (b) Fluid manipulation steps. The growth of a gel bar with embedded particles at the interface between the streams of a calcium and an alginate solution (A) is interrupted by introducing separation buffer (SB)(B). After exchanging the alginate solution (C) and removing the separation buffer, a new gel layer is formed.

all the alginate solutions are connected directly to the chip and the number of separate inlets is increased correspondingly, would allow to reduce the exchange time even more. However, in this case a switch for each solution would be necessary. A short exchange time would, for instance, be particularly advantageous when working with cells.

The procedure for forming lamellae is sketched in Fig. 3(b). First a narrow gel strip is grown, as described in Sec. III A. When the desired width has been reached, the separation buffer is injected between the gel bar and the alginate flow, and the gel growth interrupted (B). While the buffer flow is maintained, the alginate solution is exchanged for a new one with a different particle sort. The new alginate solution is introduced with the same pressure to prevent the suppression of the separation flow and the contact between the alginate and gel, before the alginate solutions have been completely exchanged (C). When all previous beads have been rinsed out and solution exchange is complete, the separation buffer is switched off and the gel growth resumes, as

soon as the alginate flow touches the gel (A′). A new layer of gel with a composition different from the initial strip is formed. Multiple layers are created by repeating these steps.

The image series of Fig. 4 is taken from an experiment (see video 3) and illustrates the formation of a single gel layer of defined width during the preparation of a multilayer gel bar. In Fig. 4(a), gel growth has been stopped with the aid of the blue separation flow, and the alginate solutions—that from which the gel top layer has been made and that for the layer to come—are being exchanged with each other. When the exchange process has finished, the separation buffer is removed (b), and the alginate containing yellow-green fluorescent beads solidifies upon contact with the gel border (c). Propagation of the gel is stopped and the borders of the new layer are defined by introducing the separation flow [(d) and (e)]. Figure 4(f) shows the corresponding fluorescence image of the gel bar with two layers more than in Fig. 4(e) and a total of ten layers. This technique offers high flexibility in gel structuring, as it allows to arbitrarily vary the number and sequence of the gel layers as well as their width and composition.

Another layered gel bar is shown in Fig. 5, where a thin layer with 30 μm width is indicated. It will be shown in the following that this value is on the order of the smallest width attainable under the given conditions. The rationale is done under the premises that gel width increases only by the re-action of alginate with the calcium that diffuses through the gel and that variation of gel width by expansion or shrinkage, which could be induced upon a change of the liquid environment, e.g., when the separation buffer is introduced, is disabled. Both conditions are assured with firm adherence of the gel to the channel walls.

In order to control and also to minimize the width of a layer, gel growth needs to be interrupted immediately. This is achieved by detaching the alginate flow from the gel by means of the separation buffer. It is also conceivable to detach the calcium flow by introducing the separation flow from the inlet which has been plugged [see Fig. 1(b)]. However, in this case the gel growth would continue until all the calcium, which is left in the gel body, has diffused out into the alginate. The calcium concentration in the gel body is then expected to decrease with time according to Fig. 6. The corresponding calcium flux from the gel into the alginate is shown in the inset. The width Δw of the gel (w is the absolute width), which is formed from the remaining calcium in the gel body, is obtained by integration of this flux,

$$\frac{\Delta w}{w} = 0.167 \frac{[\text{Ca}^{2+}]_0}{[\text{Ca}^{2+}]_{\text{gel}}}, \tag{1}$$

where $[\text{Ca}^{2+}]_0$ is the calcium concentration in the flow and $[\text{Ca}^{2+}]_{\text{gel}}$ the concentration of the chemically bound calcium in the gel. Accordingly, when taking 20 mM for $[\text{Ca}^{2+}]_0$ and a value of 50 mM for $[\text{Ca}^{2+}]_{\text{gel}}$,[36] the gel width should still increase by almost 10% when the calcium flow is detached from the gel. Hence, in order to produce fine structures, the interruption of gel growth by removal of the alginate flow is required.
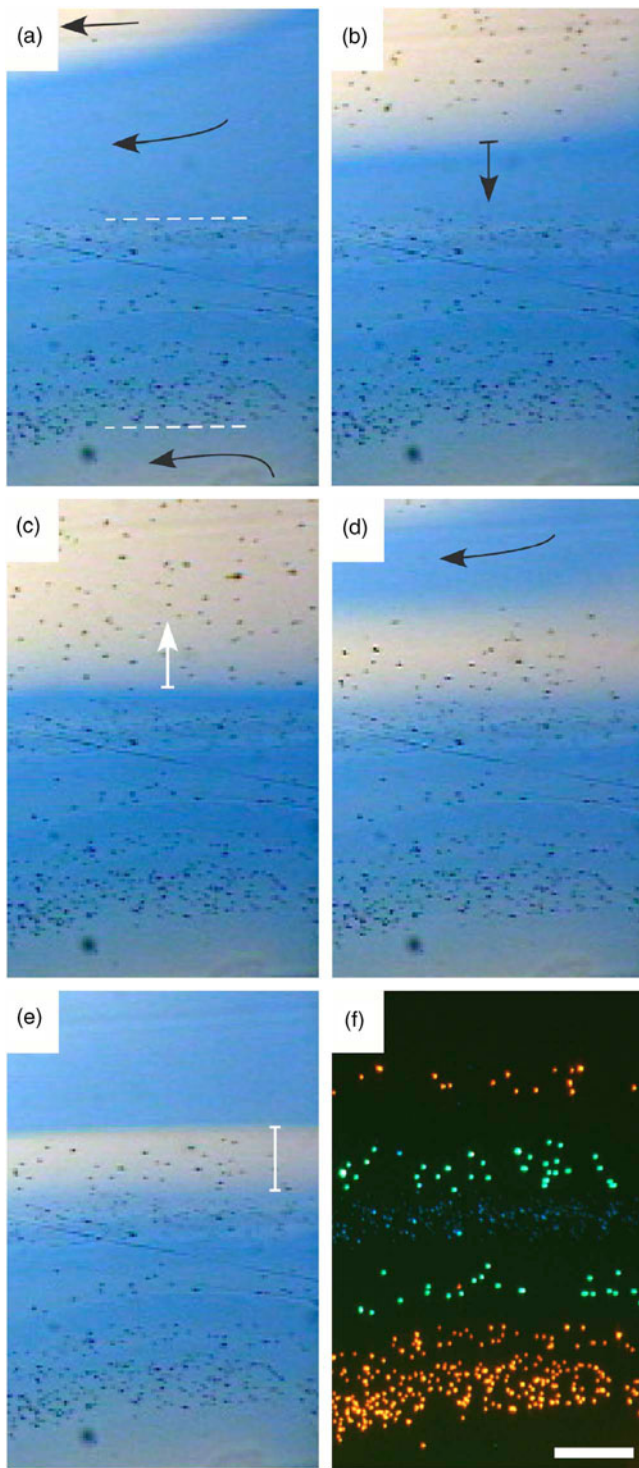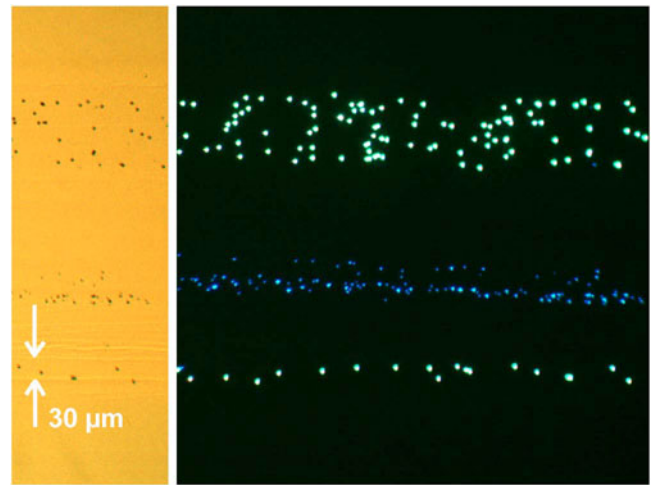
FIG. 5. Patterning of fine lamellae (left: bright field image; right: fluorescence image). With a calcium concentration of 20 mM, the smallest attainable layer width is calculated to be on the order of 10 μm. The gel was grown from top to bottom.

To estimate the smallest widths, which are enabled by this technique, two factors have to be taken into account. The first is the time it takes to stop the gel growth by introducing the separating buffer and to completely remove the viscous alginate from the gel front. The second factor is the growth rate of the gel. In Ref. 31 it has been shown that the gel growth can be satisfactorily described as a diffusion controlled process. Applying Fick's law, one can derive that the width of gel formed within a certain time span is proportional to the calcium concentration in the calcium flow,

$$\frac{\Delta w}{\Delta t} = \frac{D}{w} \frac{[\text{Ca}^{2+}]_0}{[\text{Ca}^{2+}]_{\text{gel}}}, \tag{2}$$

where D is the calcium diffusion constant in the gel. Consequently, easy control over the stripe width is obtained by

FIG. 4. Formation of a single gel layer. The image series is taken from video 3 of the supporting information. In (a) the borders of the gel bar are indicated by a pair of hatched lines and the liquid flows (just arriving from the chip entrances) by black arrows. The clear alginate solution with beads is flowing on top, the blue separation buffer beneath, and the calcium solution (20 mM) on the bottom of the image. When (b) the separation flow is removed, (c) the alginate flow gets into contact with the gel and starts to solidify growing into the alginate flow (white arrow). In (d), separation buffer is introduced again to stop the layer growth. When the alginate has been removed, (e) the freshly formed gel stripe is clearly discerned. The corresponding fluorescence image with two more layers (alginate and alginate/red beads, ten layers altogether) than in (e) is displayed in (f). The bar is 100 μm. Times (a) 0 s, (b) 14 s, (c) 29 s, (d) 142 s, and (e) 157 s.
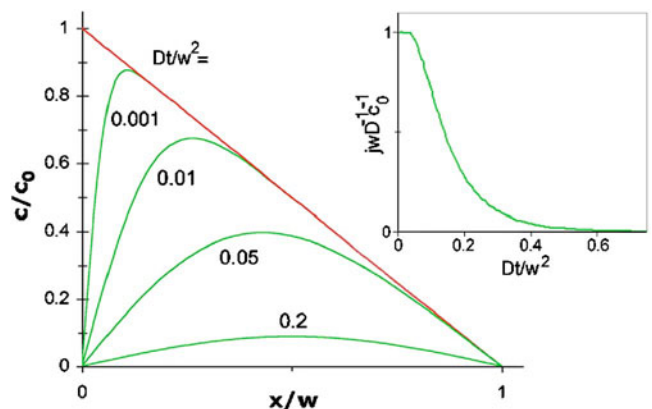
FIG. 6. Calculated decrease of the calcium concentration in the gel body (the initial distribution is shown by the red line) when the calcium flow is detached from the gel (Ca flow/gel boundary at $x=0$). The resulting calcium flux from the gel body at the gel/alginate interface ($x=1$) is shown in the inset. The plots are derived from the corresponding diffusion equation in Ref. 35. w: gel width; c: concentration of mobile Ca in the gel; c_0: Ca concentration in the flow; j: Ca flux; D: Ca diffusion coefficient in the gel; and t: time.

adjusting the calcium concentration $[Ca^{2+}]_0$, and very low calcium concentration should allow to grow an extremely thin layer of gel. The gel width w in Fig. 5 is about 500 μm and $[Ca^{2+}]_0$ is 20 mM. According to Fig. 4, the shortest time to grow a layer is nearly 30 s (see video 3). Taking 50 mM for $[Ca^{2+}]_{gel}$ and 7×10^{-10} m^2 s^{-1} for D,[36] the smallest attainable layer width Δw calculated from Eq. (2) for the present conditions is 10–20 μm.

As gel growth occurs by calcium diffusion over all the gel face, layer width is not restricted by the gel (or channel) height. This means that lamellae with extraordinarily large aspect ratios are feasible, a feature which is unique compared to other methods. With photopatterning, for instance, the resolution of gel microstructures is determined by the optical limitations (degree of depth penetration, collimation, and diffraction) and the polymer properties (reaction propagation, diffusion of radicals beyond the illuminated region, and swelling) and is compromised by the need to preserve cell vitality.[21,26,37]

B. Gel patterning by flow rate variation

It has been found that particle incorporation in the gel during growth is suppressed when the flow rate of the alginate solution is strongly increased. This has been utilized for gel microstructuring simply by flow speed variation. Figures 7(a)–7(c) illustrate the formation of a gel bar, in which three layers with high density of yeast cells are alternating with three layers of pure gel: during the growth of a gel bar with particles being embedded [Fig. 7(a)], the speed of the alginate flow is abruptly increased, which has the effect that the gel continues to grow without incorporating particles [Fig. 7(b)]. When the flow speed is reduced, the particles are trapped again. In Fig. 7(d), the gel bar is being dissolved and the embedded cells are released after introducing the EDTA solution. Figure 7(e) shows the growth curve of the gel bar during the structuring steps of Figs. 7(a)–7(c). The corresponding change of the alginate flow rate is given below. The calcium flow was kept constant. The growth curve reveals that the gel grows much quicker at low flow rates (60–100 μm s^{-1}), when layers with cells are produced, than at higher rates (>300 μm s^{-1}), when empty layers result. The respective cell density in the gel (hatched line) is found to vary oppositely to the flow rate.

Since in this experiment the calcium flow remained unchanged, strong adhesion of the gel to the channel walls is indispensable in order to withstand the pressure, which is exerted on the gel on the alginate side with increased speed of the alginate flow.

The behavior of the gel growth rate as a function of the alginate flow rate in Fig. 7(e) probably results from the pressure change accompanying the change in the alginate flow rate. The increase of pressure on the alginate side when enhancing the alginate flow rate might reverse osmosis and cause a transport of water from the alginate through the gel, which is impermeable for the alginate molecules, reducing the amount of calcium arriving from the opposite side and consequently gel growth rate. Another reason could be that
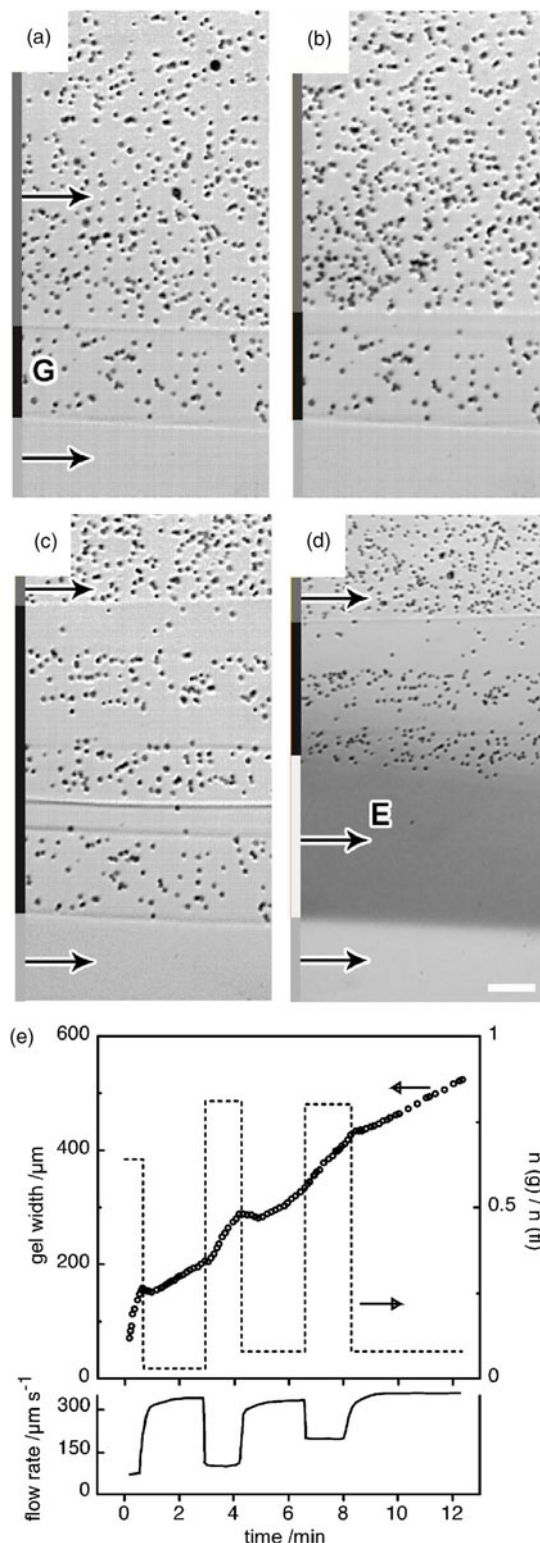

FIG. 7. [(a)–(c)] Gel microstructuring by flow speed variation. Depending on the flow rate of the alginate, particles (yeast cells) are either incorporated or excluded from the gel (G) as it grows. The arrows indicate the flow directions. The flow rate of the calcium solution (40 mM) was kept constant. Reversibility of particle immobilization is illustrated in (d), where the gel is dissolved upon feeding in EDTA solution (E). The bar in (d) is 100 μm [the scale in (d) is slightly different from (a)–(c)]. (e) The gel growth rate (open circles) is influenced by the flow rate of the alginate (below), and the cell density in the gel $n(g)$ [hatched line, normalized against the density in the solution $n(fl)$] varies oppositely to the flow rate.

the gel is compressed at the gel-alginate border by the pressure becoming thus less permeable for the calcium ions. The rise of gel growth rate each time the flow speed is dropped indicates reversibility of this process.

The alginate flow rate in Fig. 7(e) was increased or reduced rapidly to a value where exclusion of particles from or their incorporation into the gel was noticed. The values of flow rate in Fig. 7(e) are therefore arbitrary and do not necessarily coincide with the thresholds, below which cells are embedded in the gel (low rates) or beyond which the cells are excluded from the gel (high rates). There may be a narrow transition range or a definite point of transition from particle incorporation to particle exclusion situated between the low and high flow rates in Fig. 7(e). If there is a transition range, it is conceivable that therein the density of incorporated particles varies gradually with the alginate flow rate. The nature of the transition and the dependence of particle entrapment probability on alginate type and concentration, calcium concentration, the alginate flow rate or particle speed, and possibly the particle surface properties are interesting subjects to be investigated.

IV. CONCLUSIONS

Controlled algination and particle encapsulation on a microfluidic chip can be done with relatively simple and readily available equipment. Feasibility and versatility of this method are demonstrated in the present work by the manufacture of microstructured gel slabs with lamellar architecture. Width and composition of a lamella are individually variable, and with the choice of proper conditions lamellae with extremely small widths and large aspect ratios are attainable. The maximal size of a gel slab derives from the physical prerequisite to be able to produce laminar flows. This condition is fulfilled for channel heights and hence gel thicknesses on the order of a millimeter for the small flow rates applied. For the gel width there is no limiting condition. With the second technique introduced particle patterning in the gel is achieved by alternating the speed of the particle carrying flow between two extreme values. This procedure is based on the phenomenon that the capability of the gel to capture particles from the flow is dependent on the speed of the fluid. Whether this effect is related to the speed of the particles, to the growth rate of the gel, or to the gel density is yet to be elucidated.

An envisaged application of the presented techniques is the fabrication of high density gel micropatterns embedding a number of different cell types for drug screening, drug release, or cell culture studies.[38] The geometry with the particles or cells immobilized in the microchannel center and the fluid streams on either side of the gel is very advantageous for such purposes.[25] A prospect for the near future is the extension of the present technique to pattern gels in both vertical and horizontal directions.

ACKNOWLEDGMENT

[1] G. M. Eichenbaum, P. F. Kiser, S. A. Simon, and D. Needham, Macromolecules **31**, 5084 (1998).
[2] M. L. Kraft and J. S. Moore, J. Am. Chem. Soc. **123**, 12921 (2001).
[3] G. Gerlach, M. Guenther, J. Sorber, G. Suchaneck, K.-F. Arndt, and A. Richter, Sens. Actuators B **111–112**, 555 (2005).
[4] M. J. Bassetti, A. N. Chatterjee, N. R. Aluru, and D. J. Beebe, J. Microelectromech. Syst. **14**, 1198 (2005).
[5] M. E. Harmon, D. Kuckling, and C. W. Frank, Langmuir **19**, 10660 (2003).
[6] S. Nayak and L. A. Lyon, Chem. Mater. **16**, 2623 (2004).
[7] E. A. Moschou, S. F. Peteu, L. G. Bachas, M. J. Madou, and S. Daunert, Chem. Mater. **16**, 2499 (2004).
[8] D. J. Beebe, J. S. Moore, Q. Yu, R. H. Liu, M. L. Kraft, B.-H. Jo, and C. Devadoss, Proc. Natl. Acad. Sci. U.S.A. **97**, 13488 (2005).
[9] M. E. Harmon, M. Tang, and C. W. Frank, Polymer **44**, 4547 (2003).
[10] H. Suzuki, T. Tokuda, and K. Kobayashi, Sens. Actuators B **83**, 53 (2002).
[11] S. Song, A. K. Singh, T. J. Shepodd, and B. J. Kirby, Anal. Chem. **76**, 2367 (2004).
[12] A. T. Woolley and R. A. Mathie, Anal. Chem. **67**, 3676 (1995).
[13] V. A. Dowling, J. A. M. Charles, E. Nwakpuda, and L. B. McGown, Anal. Chem. **76**, 4558 (2004).
[14] R. Hagedorn, Th. Schnelle, T. Müller, I. Scholz, K. Lange, and M. Reh, Electrophoresis **26**, 2495 (2005).
[15] E. Herr and A. K. Singh, Anal. Chem. **76**, 4727 (2004).
[16] R. Dhopeshwarkar, L. Sun, and R. M. Crooks, Lab Chip **5**, 1148 (2005).
[17] S. Song, A. K. Singh, and B. J. Kirby, Anal. Chem. **76**, 4589 (2004).
[18] G. H. Seong, W. Zhan, and R. M. Crooks, Anal. Chem. **74**, 3372 (2002).
[19] W.-G. Koh and M. Pishko, Sens. Actuators B **106**, 335 (2005).
[20] A. Revzin, R. J. Russell, V. K. Yadavalli, W.-G. Koh, C. Deister, D. D. Hile, M. B. Mellott, and M. V. Pishko, Langmuir **17**, 5440 (2001).
[21] J. Heo and R. M. Crooks, Anal. Chem. **77**, 6843 (2005).
[22] A. C. Jen, M. C. Wake, and A. G. Mikos, Biotechnol. Bioeng. **50**, 357 (1996).
[23] J. L. Drury and D. J. Mooney, Biomaterials **24**, 4337 (2003).
[24] M. R. Dusseiller, M. L. Smith, V. Vogel, and M. Textor, BioInterphases **1**, P1 (2006).
[25] M. S. Kim, J. H. Yeon, and J.-K. Park, Biomed. Microdevices **9**, 25 (2007).
[26] D. R. Albrecht, V. L. Tsang, R. L. Sah, and S. N. Bhatia, Lab Chip **5**, 111 (2005).
[27] J. A. Burdick, A. Khademhosseini, and R. Langer, Langmuir **20**, 5153 (2004).
[28] N. Zaari, P. Rajagopalan, S. K. Kim, A. J. Engler, and J. Y. Wong, Adv. Mater. (Weinheim, Ger.) **16**, 2133 (2004).
[29] J. C. Zguris, L. J. Itl, W. G. Koh, and M. V. Pishko, Langmuir **21**, 4168 (2005).
[30] W. Tan and T. A. Desai, Biomed. Microdevices **5**, 235 (2003).
[31] T. Braschler, R. Johann, M. Heule, L. Metref, and Ph. Renaud, Astron. Tsirk. **5**, 553 (2005).
[32] G. Ladam, P. Schaaf, F. J. G. Cuisinier, G. Decher, and J.-C. Voegel, Langmuir **17**, 878 (2001).
[33] H. Zhu, J. Ji, and J. Shen, Biomaterials **25**, 109 (2004).
[34] S. Schneider, P. J. Feilen, V. Slotty, D. Kampfner, S. Preuss, S. Berger, J. Beyer, and R. Pommersheim, Biomaterials **22**, 1961 (2001).
[35] J. Crank, *The Mathematics of Diffusion*, 1st ed. (Oxford University Press, London, 1956), pp. 45–48.
[36] W. van Beinum, J. C. L. Meeussen, and W. van Riemsdijk, Environ. Sci. Technol. **34**, 4902 (2000).
[37] V. R. Tirumala, R. Divan, D. C. Mancini, and G. T. Caneba, Microsyst. Technol. **11**, 347 (2005).
[38] R. M. Johann, Anal. Bioanal. Chem. **385**, 408 (2006).
[39] See EPAPS Document No. E-BJIOBN-2–004702 for videos on irregular gel shape caused by weak gel adhesion. The videos may also be reached via the EPAPS homepage (http://www.aip.org/pubservs/epaps.html) or from ftp.aip.org in the directory /epaps/. See the EPAPS homepage for more information.